

Proceedings of International Collaboration on Advanced Neutron Sources (ICAMS-VII), 1983 September 13-16
Atomic Energy of Canada Limited, Report AECL-8488

STATUS REPORT OF THE SIN NEUTRON SOURCE (SEPTEMBER 1983)

F. Atchison and W.E. Fischer for the
Project Group
Swiss Institute for Nuclear Research
CH-5234 Villigen, Switzerland

INTRODUCTION

This report is in two parts. Part I describes the construction work for Injector II, which is scheduled for first beam tests later this year. Part II presents the status of the spallation neutron source (SINQ) which is planned to become operational after commissioning of Injector II and necessary improvements to other parts of the SIN-facility for the high currents.

with a 100 to 150 μA proton beam for routine operation. During 1982 a total of $455 \cdot 10^3 \mu\text{Ah}$ were delivered on target with an average beam current of 119 μA and an availability of 92 %.

Injector II is designed to deliver a beam current of at least 1 mA and consists of an 860 keV Cockcroft-Walton pre-accelerator and an isochronous cyclotron for acceleration to 72 MeV.

PART I
THE ACCELERATOR SYSTEM AND LAYOUT
OF EXPERIMENTAL FACILITIES

1. INTRODUCTION

The proposed layout of the accelerator system and experimental facilities following commissioning of Injector II are shown in Fig. 1. The site for SINQ is in the prolongation of the proton channel after the two meson targets. The guide-hall for cold neutrons is not yet included on the diagram.

At present Injector I feeds the Ring Cyclotron

2. INJECTOR II

2.1 The ion-source and pre-injector

The ion-source is of the 'multi-cusp' type: During tests, this has delivered a beam current of 40 mA, of which 40 % consisted of protons. Injector II will accept about 10 % of the current using injection without pre-bunching. A buncher could improve this ratio, but will, however, lead to a worsening of the injected beam quality.

The ion-source and acceleration tube are connected by a 60 keV beam line (ion-source extraction voltage), which contains two

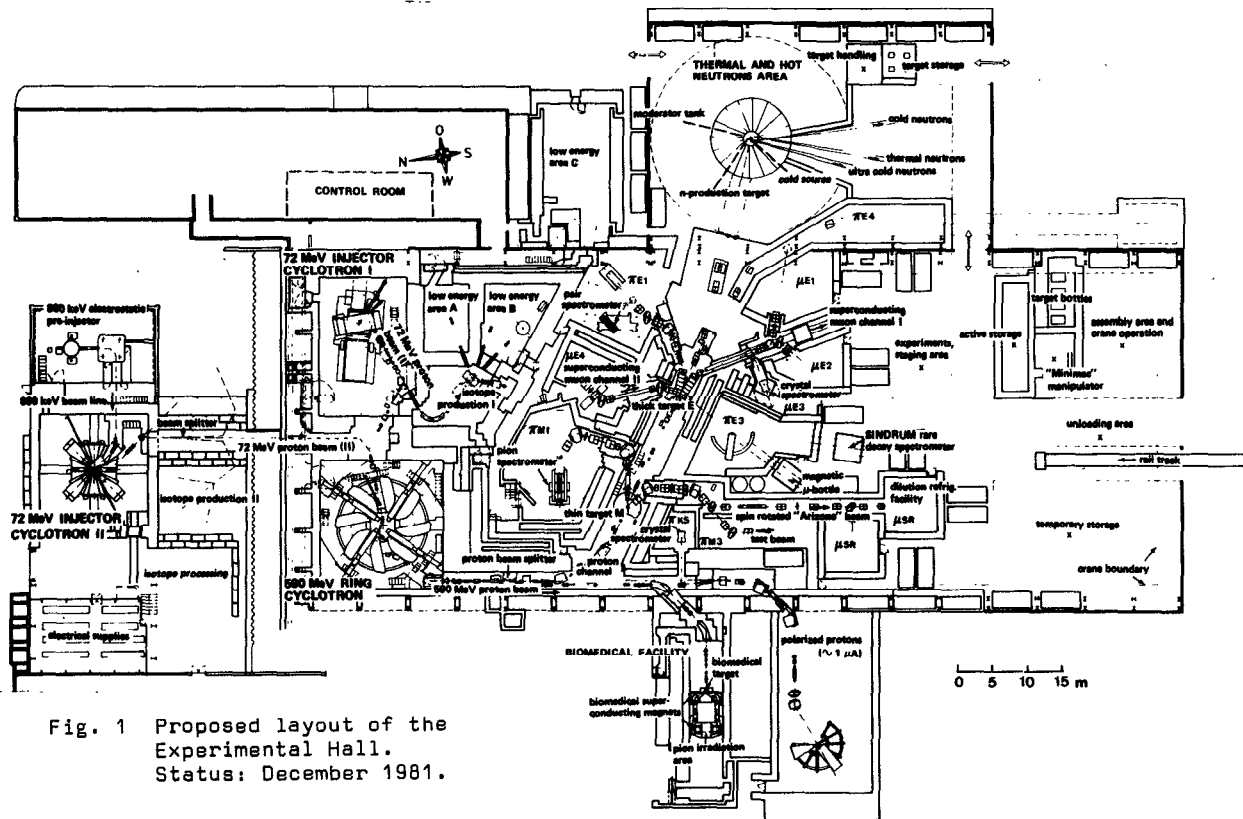


Fig. 1 Proposed layout of the Experimental Hall.
Status: December 1981.

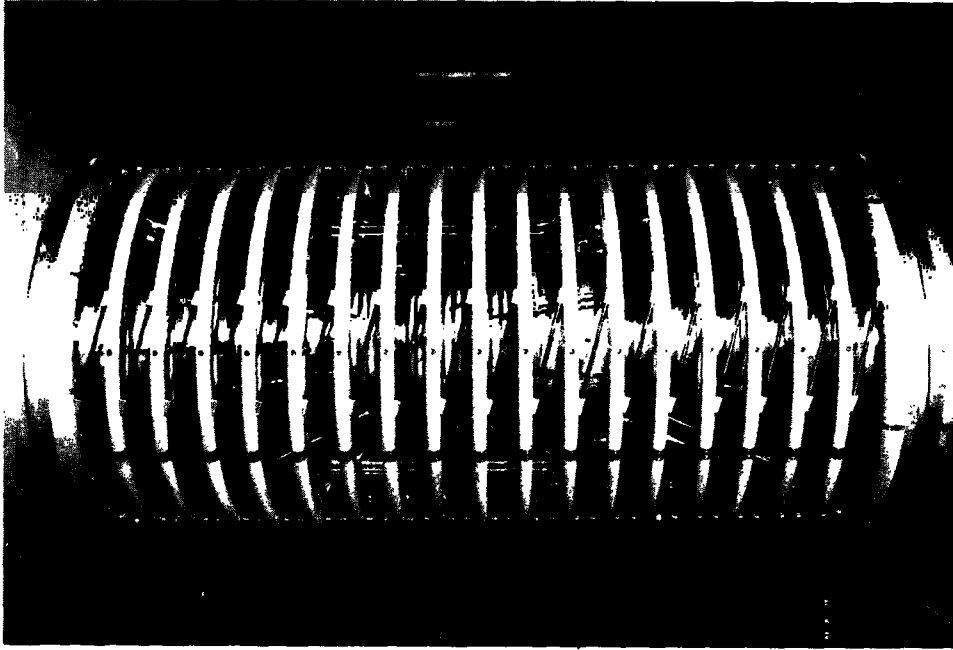


Fig. 2 The 800 keV acceleration tube installed at the Cockcroft Walton.

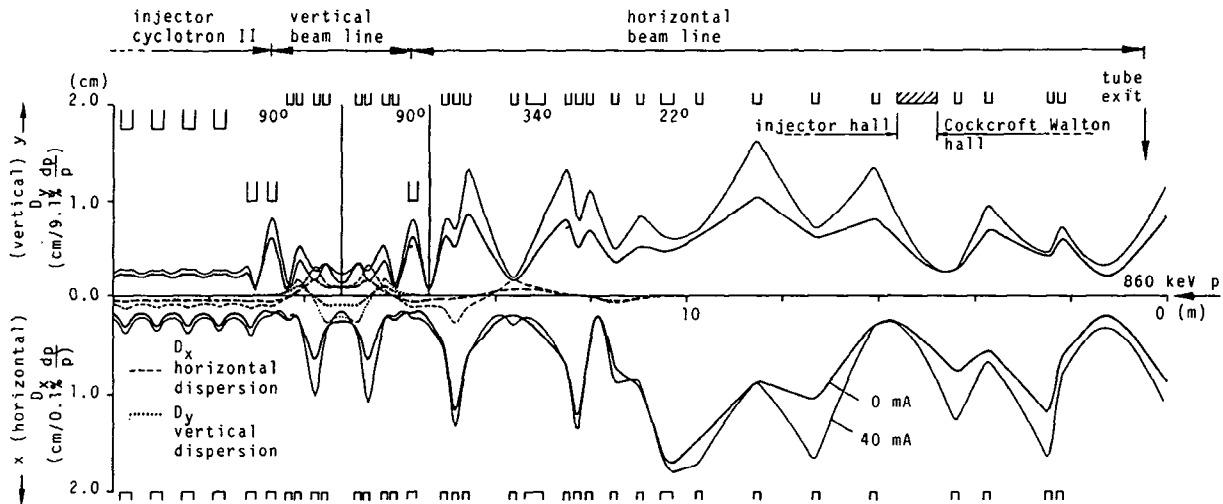


Fig. 3 Beam envelope and dispersion trajectories at 0 and 40 mA beam current in the 860 keV injection line.

solenoids and a diaphragm to remove most of the unwanted ions.

To transport this 60 keV beam, neutralisation of the space charge is essential. The neutralisation is a stationary state of a dynamic process: Electrons produced by collisions with residual gas atoms, are captured in the beam potential. These electrons are heated by the beam and diffuse back out of the potential¹. Hence the stationary state electron density (and hence neutralisation) depend on the beam energy and current and the residual gas pressure. The 60 keV beam was shown to be more than

99 % neutralised at a pressure of about 10^{-5} Torr.

A photograph of the 800 keV acceleration tube, which was installed in summer 1983, is shown in Fig. 2.

2.2 The 860 keV beam line

There were two principle problems to be solved for the design of this beam line:

- (a) Space charge: The neutralisation of the beam due to free electrons from collision is assumed to be weak and the space charge

effects from the full current will be felt.

- (b) Since the beam incorporates both horizontal and vertical bends for axial injection, the matching of the beam emittance and the dispersions to the accelerator acceptance involves eight parameters.

Fig. 3 shows the beam envelope and dispersion trajectories at 0 mA and 40 mA, for the injection line from the acceleration tube exit to the first turn in Injector II. As can be seen, the matching depends on the intensity. This leads to the necessity of four quadrupole doublets in the vertical section just before injection. This part of the line is shown in Fig. 4.

The excitation for all quadrupoles will be beam current dependent, and will be adjusted automatically by the control system.

The part of this 860 keV beam line above Injector II may be seen in Fig. 5.

2.3 The 72 MeV cyclotron

This is an isochronous cyclotron with injection and extraction radii of 33 and 300 cm in the valley of the magnetic field. The guide field and focussing is provided by 4 sector magnets (see Fig. 5), each with the following parameters:

Weight	180 t	parameters:
Pole-gap	35 mm	
Magnetic field	10.4 kG (inner radius)	
	10.9 kG (outer radius)	
Power consumption	34 kW	

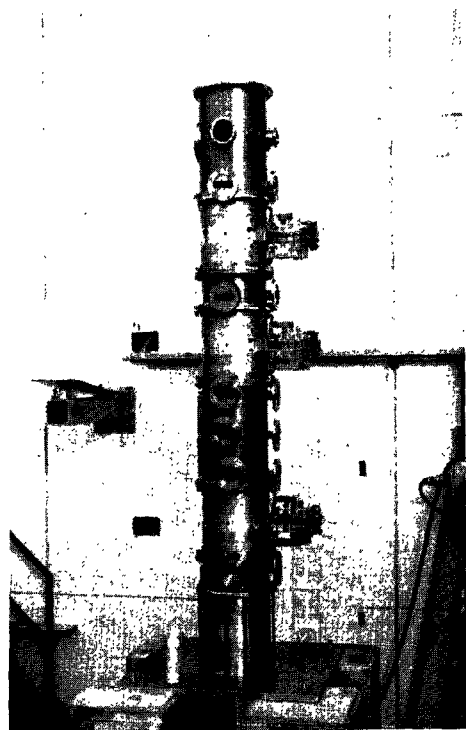


Fig. 4 Vertical insert for axial injection into the cyclotron. It contains eight quadrupoles and boxes for diagnostic elements.

Acceleration is provided by two 50 MHz $\lambda/2$ -resonators each having two acceleration gaps. The power consumption is 150 kW per resonator. In order to obtain phase compression of the bunches during the whole acceleration time, the acceleration voltage increases from 125 kV/gap at the injection radius to 250 kV at extraction. Explanation of this effect may be found in reference 2.

By adding a third harmonic to the 50 MHz, and making a proper choice of amplitude (100 kV), the energy spread of the beam at extraction may be minimised. A 150 MHz cavity positioned between two of the sector magnets may be seen in Fig. 5. By adjustment of the phase between the fundamental and third harmonic, longitudinal space charge effects may be compensated to first order.

All these measures lead to a 'straightening' of the particle bunches in the cyclotron, to create clearly separated turns, which is essential for a good extraction efficiency.



Fig. 5 A view of the 72 MeV cyclotron, also showing part of the injection line.

PART II THE NEUTRON SOURCE

1. INTRODUCTION

The present medium term plan for the SIN experimental program, shows the SINQ neutron source ready for operation in 1988. Money for construction should become available in late 1985; to meet this timetable, detailed engineering design work should commence in the early part of next year (1984).

2. THE TARGET

2.1 General

The production target is to be a vertical cylinder with a 20 cm diameter and 3 to 4 m length, of Pb/Bi eutectic mixture in the liquid phase. The design aim is to employ natural convection to transfer the beam heat about 3 m upwards. This allows three principal advantages; (i) no mechanical pumps for the liquid metal; (ii) the heat-exchanger and first conventional cooling circuit are removed well away from the high radiation field; (iii) the avoidance of complication and space conflicts, from cooling circuitry close to the neutron production region of the target. The 'extra' length also acts as the beam dump.

The two major concerns are the design for the proton-beam window and the thermofluid behaviour.

2.2 The beam window

With the expected proton current (1 to 3 mA) and beam distribution, a peak proton flux of 2 to $6 \cdot 10^{14}/\text{cm}^2/\text{sec}$ will be incident on the window. This is accompanied by a fast and HE neutron flux of 1 to $3 \cdot 10^{14}/\text{cm}^2/\text{sec}$. The window has to support a 'hydrostatic' pressure from the Pb/Bi which is 3 to 4 bar, and be corrosion resistant to the Pb/Bi. Ideally the window will be cooled on its inner face only by the Pb/Bi.

It is most likely that the beam window will be the limiting component on the target lifetime; we aim for this to be at least 1 year.

An experiment is in progress at the Los Alamos beam dump to examine the mechanical properties of stainless steel under proton irradiation comparable to that expected in operation. The samples are also being irradiated in contact with Pb/Bi to make a first attempt at seeing if there are any radiation induced corrosion effects. There are no results yet.

2.3 Thermofluid behaviour

Theoretical studies of the thermofluid behaviour of the target completed so far^{3,4}, have concentrated on obtaining results to increase our knowledge of the processes involved in natural convection in an enclosure and driven by internally generated heat. Parameter surveys have been made which include the effect of target height, beam size and power and the effect of sidewall cooling.

Targets with aspect ratio (height/diameter) up to 15 and beam current to 1 mA have been examined. These calculations may be summarised as follows:

- (i) The Pb/Bi flow shows a simple total circulation throughout the target following establishment of the steady state, in all cases studied.
- (ii) The maximum temperature at the steady state and the deposited energy show a simple power law relationship (Fig. 6).

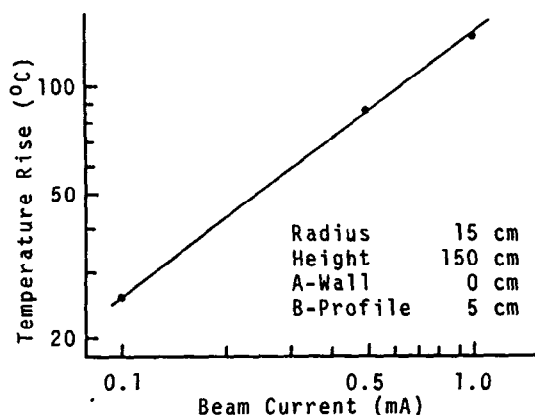


Fig. 6 Maximum temperature rise in the target as a function of beam current.

- (iii) There is no need to cool the lower 1 m of the target (in the region of the moderator) as long as sufficient area is available for heat transfer in the region above.

More detailed aspects of the thermofluid behaviour are given in a separate report to this meeting by Takeda⁴.

The theoretical studies are being backed up with an experimental program, leading eventually to a full scale test including Pb/Bi. The first large scale test-rig is now in operation and is shown in Fig. 7. These initial tests are being made with water; preliminary results may be found in⁴.

2.4 Target activation

The effect of fission on target activation has been examined. The calculated fission probability is 0.09/proton and leads to the mass distribution shown in Fig. 8. In terms of gross activation and decay power the effect of fission is small. There are two principal effects; the production of nuclides in the 50 to 150 mass region; the production of delayed neutrons.

In terms of overall neutron-source safety, the production of Kr, Xe and Iodine are of particular note: The 'hazard rating', based on potential ingested dose without holdback factors, for Iodine is greater than that for Hg, one of the most populous products, but is about three orders of magnitude below Po-210. Both Po and Iodine will be a major consideration in the design of containment systems.

The delayed neutron precursor activation is about 230 Ci, corresponding to $8.4 \cdot 10^{12}$ n⁰/sec, the flow velocity of the Pb/Bi (60 cm/sec) and short half life (0.2 sec up to 1 min), lead to about $5 \cdot 10^{10}$ n⁰/sec at the top of the target.

The decay-power and energy release as a function of time after 1 year of irradiation at 1 mA, is shown in Fig. 9. The thermal capacity of the target is about 0.15 MJ/°C, hence after



Fig. 7 General view of the thermofluid dynamics test-rig.

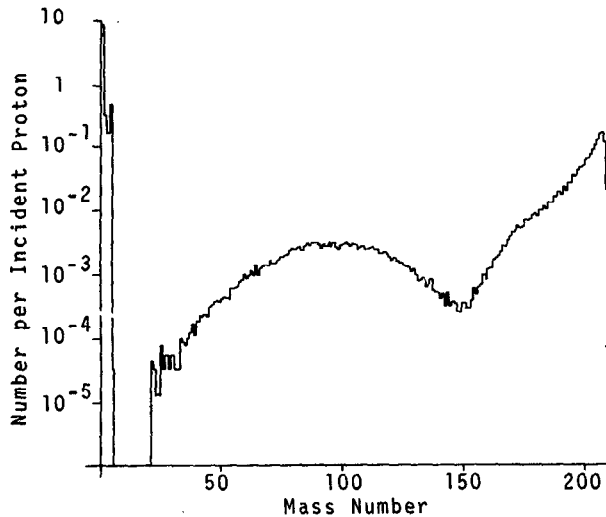


Fig. 8 Mass distribution for 590 MeV proton bombardment of Pb/Bi including fast fission.

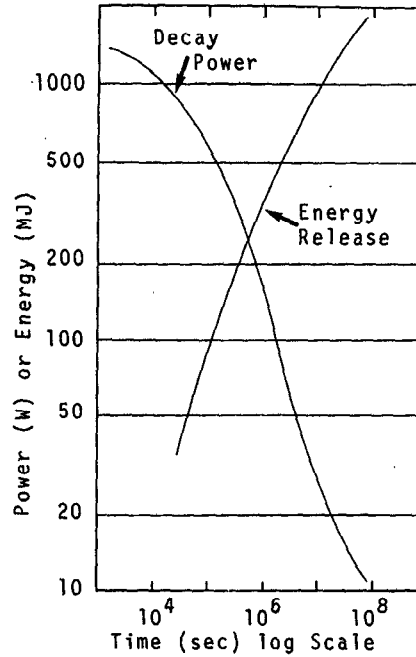


Fig. 9 Decay power and accumulated energy release from the decay of spallation product activity following 1 year irradiation at 1 mA.

1 day, a totally thermally isolated target will have a temperature rise of about 490° C. If cooling at the 0.5 kW level is maintained, the maximum temperature rise in the system is limited to about 270° C.

2.5 Vapour pressure above Pb/Bi surface

There will need to be an interspace above the Pb/Bi surface to accumulate the gaseous products. The hydrogen and helium will be accompanied by gaseous fission products and the vapours from (principally) Hg and Po. First estimates for Hg and Po using the methods of Hellwig et al.⁵, give the following results for a 15 cm radius free surface.

- (i) Mercury. Of the ~78 kCi at equilibrium, about 76 % (49 kCi) will be liberated at a temperature of 200° C; this rises to 87 % (67 kCi) at 325° C.
- (ii) Polonium. The equilibrium activity is about 5 kCi and produced via the channel $^{209}\text{Bi}(n,\gamma)^{210}\text{Bi}$ followed by β -decay. The released activity and evaporation rates ($\text{g}/\text{cm}^2/\text{sec}$) as a function of temperature are as follows:

T(°C)	Activity (Ci)	Evap. Rate
177	0.0007	$1.3 \cdot 10^{-17}$
227	0.04	$7.0 \cdot 10^{-16}$
277	1.1	$2.0 \cdot 10^{-14}$
327	19.0	$3.4 \cdot 10^{-13}$
377	200.0	$3.6 \cdot 10^{-12}$

3. THE MODERATOR

3.1 General

Tritiation of the D_2O is a known and expected consequence of source operation. The estimated activation levels are 0.8 Ci/litre at one year, 2.3 Ci/litre at three years and an equilibrium activity of 14.4 Ci/litre.

To limit corrosion and to remove gas (mainly from dissociation of the D_2O) a processing plant will be required. The plant is to consist of resin beds and degassing equipment; at this stage we do not plan to include catalytic recombiners. In view of the need to have continuous processing and a pumped D_2O circuit, we now plan to incorporate the moderator heat exchanger into this system.

3.2 Cold source I: General

There are two possibilities for the cold source, (i) a large volume of D_2 or (ii) a small grooved H_2 -type. Values from⁶ show an optimal D_2 -source to have a 50 % to 100 % higher gain factor compared with an optimal H_2 source. Recent measurements at Orphée⁷ show higher gain factors than in reference 6; also the results of Inoue et al.⁸ show a doubled gain factor for a grooved compared to an ungrooved methane source. These results would indicate that a grooved H_2 source could have a performance at least as good as for D_2 .

As available refrigeration power is enough for two small H_2 sources and this leads to a more satisfactory overall source layout, the relative performance of these two cold source types with the SINQ geometry is to be measured experimentally by the KFA-SIN-TU Munich collaboration, in an experiment starting in the first half of next year (1984).

3.3 Cold source II: Heat deposition

Results from the recent heat deposition measurements made at TRIUMF⁹, allow new estimation of the expected power. Heat generation in H_2 and D_2 were deduced to be 36 and 19 mW/g, and for Al (a probable construction material) measured as 1.9 mW/g.

For a 1 litre H-source with a 5.0 mm thick spherical Al shell container, the estimated total heat load is 419 W/mA, the principal contributions being 224 W in H and 133 W in Al from fast neutrons and γ 's; 37 W in H_2 , and 25 W in Al from neutron capture.

For the D_2 source, a volume of about 20 litres will be required. Again using a spherical geometry, the large size requires taking the neutron flux variation into account. The heat distribution for the D_2 along the diameter perpendicular to the target and in the Al shell, are shown in Fig. 10. The fast neutron contribution dominates and is based on the flux distribution:

$$\phi = r^n \cdot \text{Exp}(-\lambda r)$$

By fitting to diffusion calculation results, values of $n = -1.3$ and $\lambda = 0.021/\text{cm}$ were obtained.

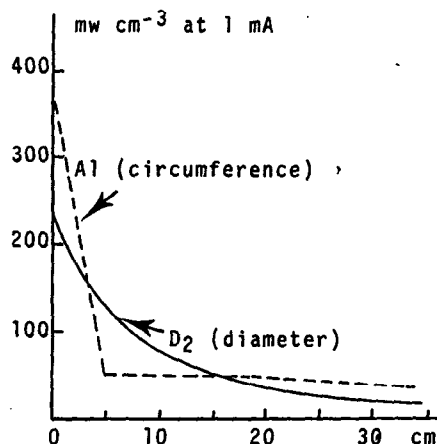


Fig. 10 Power deposition in the wall and D_2 for a 20 litre D_2 cold source.

Approximate integration of the power distribution gives a value of about 1.5 kW/mA. Fig. 10 also shows that this relatively large power may be reduced considerably by removing the cap beside the target, if this should turn out to be neutronically ineffective.

4. OVERALL SOURCE LAYOUT

4.1 General

A plan view of a preliminary version of the SINQ layout is shown in Fig. 11 and a vertical cut, in the central region of the source, in Fig. 12.

We plan to make the beam-tube tips replaceable as the possibility of failure of a beam-tube window cannot be entirely excluded. The central column containing the target and proton beam entrance line (see Fig. 12) will be subject to similarly high radiation damage and this is also planned to be replaceable. Collimators will be mounted in this central column; carbon in the region of the moderator and iron below. These are necessary to limit the consequences of a proton beam mis-steer.

Target extraction is from the top and will be made directly into a transport flask. The top plug can also be removed, allowing in principle replacement of the D_2O tank. The use of a light water layer outside the D_2O to increase the thermal flux¹⁰ is now considered unwise in view of the consequences of leakage.

Three layers of containment are envisaged: (a) Outside the D_2O tank to contain any spillage as might occur with a beam-tube window failure. (b) An underpressure He atmosphere for the inner part of the shield. (c) An underpressure air system just outside the He containment, this air to be extracted via the proton beam tunnel ventilation system.

4.2 Beam tube layout

Current plans for the scattering facilities include both cold and thermal beam tubes, cold guides and thermal guides. The geography of the SIN site constrains the angle between the proton beam and thermal-guide bundle. There is sufficient room to accommodate guides up to about 150 m long.

There are two principle constraints to the layout of the beam-tubes; (i) their axes should be close to tangential to the target; (ii) we need to be able to replace the tips.

The thermal flux distribution allows use of two vertically displaced beam-tube layers and overall, six pairs of beam tubes are incorporated in the latest version. It is not clear that all twelve beam-ports could be used simultaneously as this depends on monochromator design and types of instruments.

Two cold sources are shown, both small H_2 rather than the single large D_2 of earlier versions: With slight changes, the two cold tube pairs and the cold-guides can be accommodated onto a single D_2 source.

One beam tube pair (HO2) could be available to view a hot-source if there is a requirement for such a facility.

4.3 Bulk shield

The source requires 4 m of iron and 1 m of concrete for the main biological shield. The first layer will require water cooling and we plan to include the inner 20 to 40 cm inside the moderator tank and use the D_2O for this. In view of corrosion problems, this first layer may be built from Pb.

Access for changing the beam tube tips will need to be through the bulk shield. Minimisation of the shield thickness is particularly relevant for the beam tubes. As the question of background is also intimately linked, we are investigating ways of building in as much flexibility as possible. Two schemes are under consideration:

In the first (Fig. 11), we provide 'user' boxes allowing mounting of collimators, monochromators etc. starting from a nominal 3 m radius. The size of box shown is based on the inclusion of a particular type of monochromator and would be determined in any final version by better consideration of the equipment to be mounted.

The second scheme (Fig. 12), is to provide a fixed part of the bulk shield at about 4 m radius, with full containment and no access for user equipment. The outer shielding would be built up from 'loose' blocks built up around the collimators, monochromators, etc.

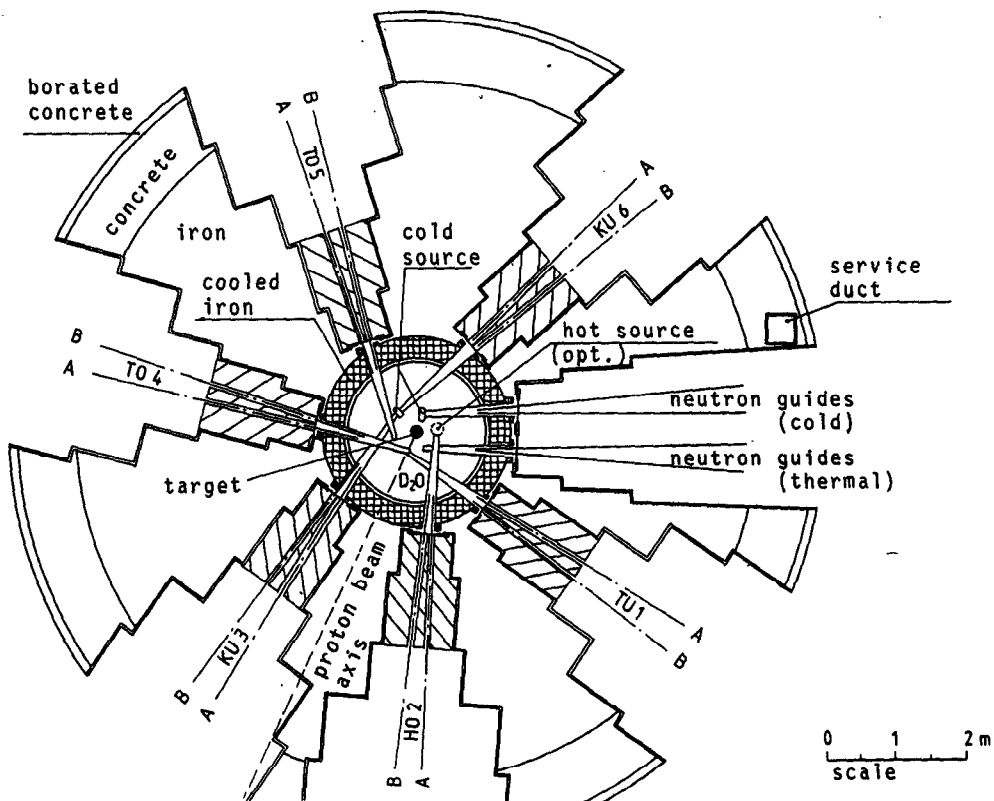


Fig. 11 A plan view of SINQ.

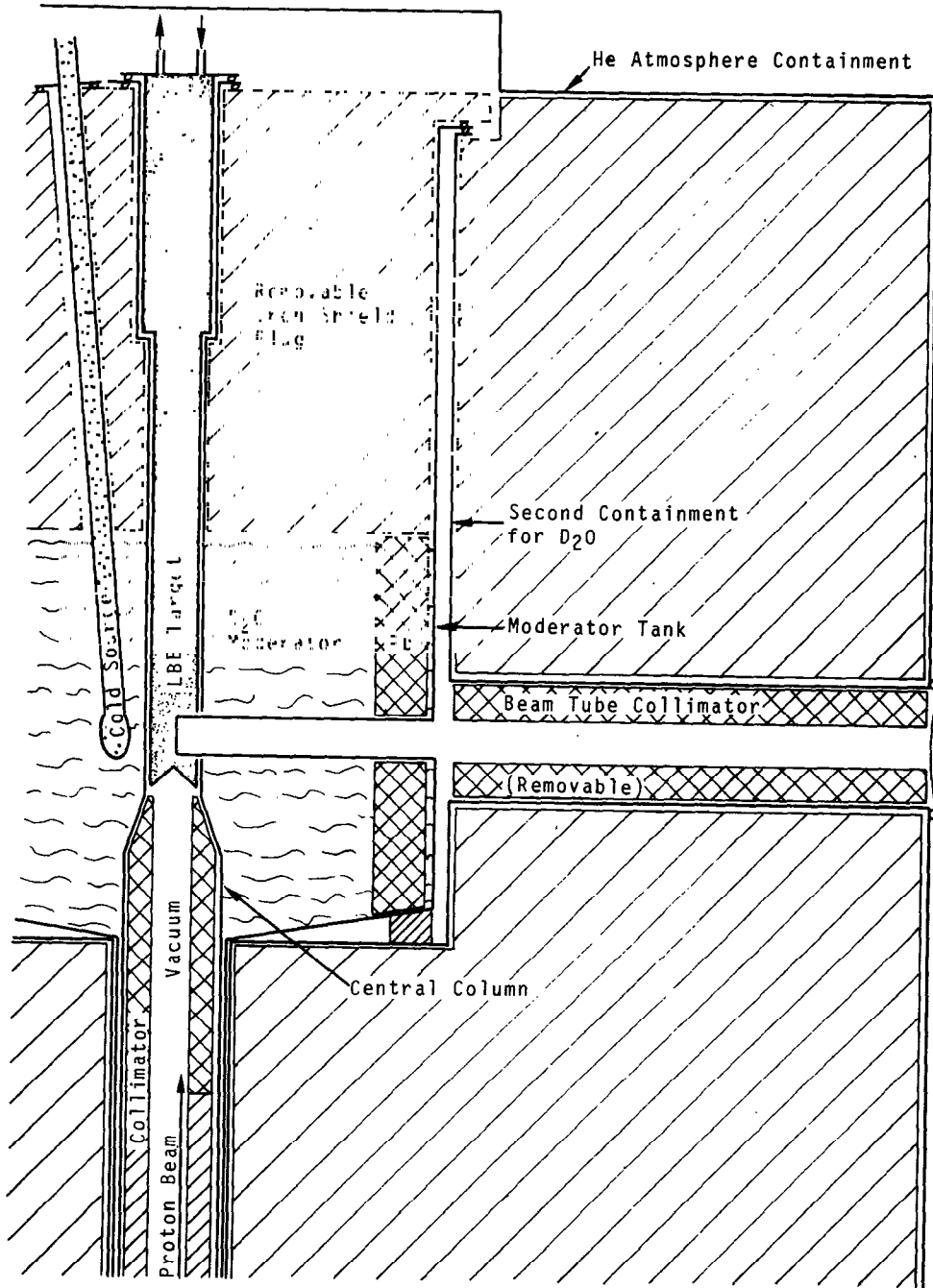


Fig. 12 A vertical cut through the central region of SINQ.

REFERENCES

1. A.J.T. Holmes, Phys. Rev. A19, 389 (1979)
2. W. Joho, Part. Accel. 6, 41 (1974)
3. Y. Takeda, Proc. ICANS-VI, 357 (1982)
4. Y. Takeda, These Proceedings
5. L. Hellwig et al., Realisierungstudie SNQ, Teil III, Annex I, JÜL-Spez-113 (1981)
6. H.D. Harig, Thesis, University of Grenoble (1967)
7. D. Cribier, Private Communication (1983)
8. K. Inoue et al., Proc. ICANS-VI, 391 (1982)
9. W.E. Fischer et al., SIN preprint PR-83-09 (1983)
10. F. Atchison et al., Proc. ICANS-VI, 441 (1982)